(2)

David Taylor Research Center

Bethesda, Maryland 20084-5000

CDNSWC/SHD-1348-01 April 1992

Ship Hydromechanics Department
Departmental Report

Bubble Dissolving in Turbulent Pipe Flow

by
Scott Gowing

Approved for public release;
distribution is unlimited

CDNSWC/SHD-1348-01 April 1992 Bubble Dissolving in Turbulent Pipe Flow

MAJOR DTRC TECHNICAL COMPONENTS

CODE 011 DIRECTOR OF TECHNOLOGY, PLANS AND ASSESSMENT

12 SYSTEMS DEPARTMENT

14 SHIP ELECTROMAGNETIC SIGNATURES DEPARTMENT

15 SHIP HYDROMECHANICS DEPARTMENT

17 SHIP STRUCTURES AND PROTECTION DEPARTMENT

19 SHIP ACOUSTICS DEPARTMENT

27 PROPULSION AND AUXILIARY SYSTEMS DEPARTMENT

28 SHIP MATERIALS ENGINEERING DEPARTMENT

DTRC ISSUES THREE TYPES OF REPORTS:

1. **DTRC reports, a formal series,** contain information of permanent technical value. They carry a consecutive numerical identification regardless of their classification or the originating department.

2. **Departmental reports, a semiformal series,** contain information of a preliminary, temporary, or proprietary nature or of limited interest or significance. They carry a departmental alphanumerical identification.

3. **Technical memoranda, an informal series,** contain technical documentation of limited use and interest. They are primarily working papers intended for internal use. They carry an identifying number which indicates their type and the numerical code of the originating department. Any distribution outside DTRC must be approved by the head of the originating department on a case-by-case basis.

NDW-DTRC 5602/51 (Rev. 3-91)

REPORT DOCUMENTATION PAGE

1a. REPORT SECURITY CLASSIFICATION Unclassified	1b. RESTRICTIVE MARKINGS
2a. SECURITY CLASSIFICATION	3. DISTRIBUTION / AVAILABILITY OF Approved for public release: distribution is unlimited *(Continued on Reverse Side)*
2b. DECLASSIFICATION / DOWNGRADING SCHEDULE	
4. PERFORMING ORGANIZATION REPORT	5. MONITORING ORGANIZATION REPORT NUMBER(S)
6a. NAME OF PERFORMING David Taylor Research Center 6b. OFFICE SYMBOL *(If applicable)* Code 1542	7a. NAME OF MONITORING
6c. ADDRESS *(City, State, and Zip* Bethesda, MD 20084-5000	7b. ADDRESS *(City, State, and Zip*
8a. NAME OF FUNDING / SPONORGANIZATION 8b. OFFICE SYMBOL *(If applicable)*	9. PROCUREMENT INSTRUMENT IDENTIFICATION
8c. ADDRESS *(City, State, and Zip Code)*	10. SOURCE OF FUNDING

PROGRAM ELEMENT NO.	PROJECT NO.	TASK NO.	WORK UNIT ACCESSION NO.
62936N	ZR00001	ZF66412001	DN509009

11. TITLE *(Include Security Classification)*
BUBBLE DISSOLVING IN TURBULENT PIPE FLOW

12. PERSONAL AUTHOR(S)
Scott Gowing

13a. TYPE OF REPORT	13b. TIME COVERED	14. DATE OF REPORT *(Year, Month, Day)*	15. PAGE COUNT
Final	FROM_____ TO_____	1992 April	vi+37

16. SUPPLEMENTARY NOTATION

17. COSATI CODES			18. SUBJECT TERMS *(Continue on reverse if necessary and identify by block*
FIELD	GROUP	SUB-GROUP	bubble dynamics mass transfer bubble stability turbulent diffusion two phase flow deaeration

19. ABSTRACT *(Continue on reverse if necessary and identify by block number)*

Measurements are presented of bubble dissolving in turbulent pipe flow at pipe Reynolds numbers of 2x104, 1x105 and 2x105, based on pipe diameter. The mass transfer coefficient is determined and it increases with Reynolds number. The coefficient appears to be independent of bubble size for the diameter range of 20-170 μm. The mass transfer Nusselt number is determined and depends approximately on the bubbles' Peclet number to the one half power.
The values of the mass transfer coefficients are similar to those for the same size bubbles rising buoyantly in still water. Suppression of dissolving by bubble rotation is hypothesized to prevent a significant increase in dissolving for the turbulent flow regime compared to the rising bubble regime. Surfactants in the water are also suspected of slowing the dissolving rates.

(Continued on Reverse Side)

20. DISTRIBUTION / AVAILABILITY OF ABSTRACT	21. ABSTRACT SECURITY CLASSIFICATION
☒ UNCLASSIFIED/UNLIMITED ☐ SAME AS RPT ☐ DTIC USERS	Unclassified

22a. NAME OF RESPONSIBLE	22b. TELEPHONE *(Include Area Code)*	22c. OFFICE SYMBOL
Scott Gowing	301-227-1410	Code 1542

(Block 19 Continued)

CONTENTS

FIGURES

TABLES

NOMENCLATURE

A	area (cm^2)
c	solute concentration (g/cm^3)
c_s	solute concentration at saturation (g/cm^3)
c_∞	bulk solute concentration far from the bubble (g/cm^3)
Δc	concentration differential (g/cm^3)
d	bubble diameter (cm)
D	molecular diffusivity (cm^2/s)
k	mass transfer coefficient (cm/s)
L_p	pipe length (cm)
m	mass (g)
n	bubble concentration (cm^{-3})
N	number of bubbles
P	pressure ($dynes/cm^2$)
P_{atm}	atmospheric pressure ($dynes/cm^2$)
P_i	absolute pressure at entrance of main pipe section ($dynes/cm^2$)
P_e	absolute pressure at exit of main pipe section ($dynes/cm^2$)
r	radial distance (cm)
R	bubble radius (cm)
R_p	pipe radius (cm)
ΔR	change of radius (cm)
t	time (s)
Δt	elapsed time (s)
U	velocity (cm/s)
$\overline{U}$	average velocity (cm/s)
U_T	terminal velocity (cm/s)
U_e	turbulence velocity scale (cm/s)

NOMENCLATURE (continued)

$\bar{\alpha}$	gas saturation level relative to bubble pressure
α_{atm}	gas saturation level relative to one atmosphere partial pressure
ϵ	power dissipated (viscous dissipation) per unit mass (ergs/s-g)
ρ	water density (g/cm^3)
ρ_g	gas density (g/cm^3)
σ	surface tension (dynes/cm)
τ_w	pipe wall shear stress ($dynes/cm^2$)
τ_s	surface tension stress ($dynes/cm^2$)
ν	kinematic viscosity (cm^2/s)
Nu	Nusselt number
Pe	Peclet number
Pe_R	Peclet number for rising bubbles
Pe_T	Peclet number for bubbles in turbulence
Re	Reynolds number

ABSTRACT

Measurements are presented of bubble dissolving in turbulent pipe flow at pipe Reynolds numbers of $2x10^4$, $1x10^5$ and $2x10^5$, based on pipe diameter. The mass transfer coefficient is determined and it increases with Reynolds number. The coefficient appears to be independent of bubble size for the diameter range of 20-170 μm. The mass transfer Nusselt number is determined and depends approximately on the bubbles' Peclet number to the one half power.

The values of the mass transfer coefficients are similar to those for the same size bubbles rising buoyantly in still water. Suppression of dissolving by bubble rotation is hypothesized to prevent a significant increase in dissolving for the turbulent flow regime compared to the rising bubble regime. Surfactants in the water are also suspected of slowing the dissolving rates.

ADMINISTRATIVE INFORMATION

This project was partly supported by the David Taylor Research Center (DTRC) Independent Exploratory Development Program (IED), administered by the Research Coordinator at DTRC Code 0012, under Program Element 62936N, Task Area ZF66412001, under Work Unit 1542-303, DN509009.

This research is a thesis for the degree of Master of Science in Ocean and Marine Engineering at the School of Engineering and Applied Science at the George Washington University. The thesis advisor was Dr. Thomas Huang of DTRC Code 1542 in coordination with Dr. James Feir at the George Washinton University.

INTRODUCTION

This thesis concerns the experimental measurement of bubble dissolving in a turbulent pipe flow. Bubbles 20 μm to 170 μm in diameter are measured at pipe diameter Reynolds numbers of $2x10^4$, $1x10^5$ and $2x10^5$. The sizes and concentrations (spectra) of the bubbles

entering and leaving a long section of tube are compared and it is found that the bubble dissolving manifests itself as a shift in the spectra along the size axis. The results are summarized in the form of mass transfer coefficients and Nusselt numbers which are compared to similar coefficients of bubble dissolving in other flow regimes.

MASS TRANSFER COEFFICIENT MEASUREMENT

The mass transfer coefficient k can be expressed as

$$k = \frac{-dm/dt}{A\Delta c} \tag{1}$$

in which $-dm/dt$ is the mass transfer rate of gas out of the bubble, A is the bubble surface area and Δc is the difference in concentration potential which drives the dissolving process. The mass transfer rate will be negative for a dissolving bubble. The bubble surface is assumed to be saturated with respect to the gas pressure inside the bubble in accordance with Henry's Law. Gas will diffuse much more slowly through the surrounding liquid than inside the bubble, hence the concentration difference across the diffusion boundary layer controls the dissolving rate. This concentration potential is

$$\Delta c = c_s - c_\infty$$

in which c_s and c_∞ are the saturated and bulk liquid gas concentrations, respectively. Equation 1 can then be rewritten as

$$k = \frac{-dm/dt}{4\pi R^2 (c_s - c_\infty)} \tag{2}$$

The continuity equation for the gas leaving the bubble is

$$\frac{dm}{dt} = 4\pi R^2 \rho_g \frac{dR}{dt} + \frac{4}{3}\pi R^3 \frac{d\rho_g}{dt} \tag{3}$$

For the pipe flow experiments performed in these tests, the second term in the equation is small compared to the first and can be ignored. Equations 2 and 3 then lead to

$$k = \frac{-\rho_g dR/dt}{c_s - c_\infty} \tag{4}$$

The coefficient k can then be determined experimentally by measuring the average value of dR/dt as the change of bubble size, ΔR, over a known period of time, Δt, calculating the gas density in the bubble, ρ_g, and measuring the dissolved gas concentration in the pipe flow, c_∞. The change in bubble size is measured by the shift along the size axis between the intake and exit bubble spectra of size versus number density or concentration.

EXPERIMENTAL APPROACH

The experiment is designed to determine the mass transfer coefficient as defined in Equation 4 by measuring the necessary parameters.

To create a pipe flow, water is pumped out of a water tunnel into a long section of flexible tube and back into the tunnel again. The tunnel serves as a large reservoir of variable air content water which can be pressurized or depressurized by the tunnel pressure control system. Located at the upstream and downstream ends of the tube are long (30 diameter minimum) sections of smooth, straight pipe of matching diameter to establish fully developed pipe flow going both in and out of the tube. The tube lies flat on a floor and is arranged in the shape of a long "U" to bring the entrance and exit sections close together. The return bend in the middle of the "U" is large in radius to maintain an essentially constant, fully developed pipe flow throughout the whole tube section. For further reference, the tube with attached pipe sections at the ends will be called the pipe section in general. See Figure 1.

Air bubbles are created in a bubble generator and injected into

the pipe upstream of the pump. A small portion of the flow is diverted at the entrance to the upstream pipe section to a bubble detector for measuring sizes and concentrations (spectra) of the bubbles going into the pipe. At the exit of the downstream pipe section, a small portion of the flow is similarly diverted to the same detector for sampling bubbles leaving the pipe.

The differences between the two bubble spectra show changes in bubble sizes caused by dissolving. Assuming that the bubbles that enter the pipe neither coalesce, breakup or dissolve completely before leaving the pipe, continuity requires that the number density of bubbles flowing through the pipe section remains unchanged. The bubbles will dissolve to a smaller size, and this effect appears as a shift in the bubble spectra along the size axis, ΔR. Assuming that bubbles of a given size all dissolve at the same rate, variations of this dissolving effect with bubble size will appear in the shift of the spectra also. For example, if 5.0 bubbles/cm^3 in the 90-100μm size range enter the pipe, then that same concentration of bubbles will exit the pipe in a smaller size range. The assumptions regarding bubble breakup or coalesence are significant and are addressed in the "Assumptions and Approximations" section.

Pipe flow parameters are measured with simple pressure taps located in the upstream and downstream pipe sections The taps are connected to a calibrated differential pressure gage for measuring pressure drop and gage pressures at the ends of the pipe section. The average pipe velocity is calculated from the equation from Schlichting (1979) relating average velocity and pressure gradient,

$$\overline{U} = \left[\left(0.0665 \rho \upsilon^{1/4} R_p^{-5/4} \right)^{-1} dP/dx \right]^{4/7} \tag{5}$$

and the pressure gradient is simply the total pressure drop divided by the length of pipe between the taps. The average velocity is used to define the pipe Reynolds number:

$$Re = 2\overline{U}R_p/\upsilon \tag{6}$$

Dividing the derived velocity into the length of the pipe from the intake bypass point to the exit bypass point yields the elapsed dissolving time, Δt.

$$\Delta t = \frac{L_p}{\overline{U}} \tag{7}$$

Dividing this value into the shift of the bubble spectra, ΔR, yields the average of the bubble shrinking rate in Equation 4, dR/dt, over the length of the pipe section.

The last parameter required to determine the transfer coefficient is the non-dimensional term that represents the air saturation level. Assuming the air in the bubble behaves like a perfect gas, ignoring surface tension contributions to the internal bubble pressure, and assuming Henry's Law for gas solubility, the remaining terms in Eq. 4 can be rewritten as

$$\frac{\rho_g}{c_s - c_\infty} = \frac{\rho_{gatm}}{c_{satm}}\left(1-\overline{\alpha}\right)^{-1} \tag{8}$$

in which ρ_{gatm} and c_{satm} are the air density and solubility in water at one atmosphere of pressure and $\overline{\alpha}$ is the average air saturation level integrated over the length of the pipe section. The average saturation value must be used for Equation 4 because the average bubble size reduction is what is measured. This average saturation value is

$$\overline{\alpha} = \frac{\alpha_{atm} P_{atm}}{P_i - P_e} \ln \frac{P_i}{P_e} \tag{9}$$

in which α_{atm} is the saturation level with respect to one atmosphere of pressure and P_i and P_e are the absolute inlet and exit pipe pressures measured with the differential pressure gage and a barometer. A manometric device that measures the percent air saturation of the water with respect to the water temperature and one atmosphere

partial pressure is used to measure the air content α_{atm}.

For the three Reynolds number conditions tested, three tests were run at different air contents to insure that there was no dependence of the results on saturation level and also to better define the transfer coefficient by three values instead of one.

Thus all the parameters for determining the mass transfer coefficient can be measured with this experimental approach.

EXPERIMENTAL EQUIPMENT

PIPE FLOW SYSTEM

A schematic of the pipe flow system is shown in Figure 1. The water tunnel to which the system is attached serves as a large reservoir of variable pressure, variable air content water with filtering capability. The water flows from the tunnel through the pipe back into the tunnel. The tunnel water is slowly circulated to resorb any bubbles that exit the pipe and provide bubble-free water going into the system.

The best way to describe the system details is to follow the water flowing through it. Water enters the pump from a 3 inch diameter pipe section that minimizes incoming friction losses. Bubbles are injected just upstream of the pump. The 65 feet head, 110 GPM pump is a single stage, centrifugal, constant speed design. The exiting flow then passes through a tee where part of the flow may be bypassed back to the tunnel. This prevents pump loading when the flowrates through the pipe section are small. Thirty diameters of straight pipe after this tee establish fully developed turbulent flow by the time the water enters the main section of the pipe system. At this point, about 10% to 40% of the flow can be bypassed through a long radius tee to the bubble detector for measuring the bubble spectrum going into the main pipe section. See Figure 1a. The bubble spectrum is assumed to remain unchanged in its short transit from the diverting tee to the detector. The length of pipe from the tee to the detector is only 2 feet and little dissolving should take place in the short time span that the bubbles transit this section. The rest of the flow goes into the main pipe section which is either a 110 foot or 55 foot long section of 2 inch I.D. PVC

tubing. The tube lengths were chosen to allow enough time for significant dissolving without complete bubble extinction. The tubing lies in an elongated U-shape and returns the flow to another tee where 10% or 40% of the flow can again be bypassed to the bubble detector. This is to measure the exiting bubble spectrum. See Figure 1b. The measured dissolving is assumed to occur between the two tees that divert the flow to the detector. The length of pipe between these tees is the length used to determine the elapsed flow time. The rest of the flow returns to the tunnel through a 3 inch pipe section that minimizes losses.

The bypass and bubble detector pipes have shutoff or flow control valves where they are required, and there is an additional valve at the exit of the main section for flow control.

The pressure and pressure drop in the main pipe section are measured with a calibrated, Bourden tube differential pressure gage or a water manometer. One side of the gage can be vented to atmosphere for gage pressure measurements. The pressure taps are two horizontally opposed 1/16 in. I.D. holes drilled into smooth PVC pipe and straight pipe extends 20 diameters upstream and 10 diameters downstream for good pressure measurements.

BUBBLE DETECTOR

The bubble detector used for these measurements is shown in Figure 2. This detector was built by Dr. S.C. Ling of Catholic University and has been used mostly for bubble measurements in water tunnels. The detector is a light scattering instrument that both counts bubbles and measures their sizes. The light source is an incandescent bulb with a condenser lens. Masks define two rectangular light beams of known section, and the mask image is focussed in the water pipe for precise sampling area definition. The receiving optics focus the image of the bubbles onto photomultiplier tubes and masks further define the sampling volume for calculating bubble concentrations. The elapsed times for the bubbles to cross the two beams, spaced apart 7 mm, provide their velocities for calculating concentrations and velocity

variations. The sampling volumes are also shown in Figure 2.

The scattered light pulses from the photomultipliers are recorded on a pulse height analyzer for pulse counting and sizing. The pulse height is proportional to bubble diameter squared and a bubble calibration curve is used to get the bubble size from the pulse data. Calibration bubbles are electrolytically generated and sized according to their terminal velocities. The terminal velocities are measured by placing the detector sideways and allowing the bubbles to float through the two sampling volumes. The water in the calibration process is treated with a small amount of surfactant to create a rigid surface on the bubble. A Stokes Law type terminal velocity relation is then used for equating bubble speed and size. The calibration curve is shown in Figure 3.

The sampling volume presents a large cross section to the flow to maximize the number of bubbles counted, yet the volume is thin to minimize double counting. The bubble velocities are measured at the same point used to size them so that pipe flow velocity profiles are not used to determine the average velocity at the pipe centerline. White light provides a relatively smooth intensity distribution across the sampling volume instead of the focussing that can occur with lasers. The light intensity variation that remains can be accounted for in the data by calibrating the detector at a position in the light beam that equals the average intensity in the light beam.

The instrument is designed to detect bubbles and ignore particles by utilizing the bright, specular reflection of bubbles to discriminate their signals from the weaker, diffuse scattering of particles. Some particle counts will still show up in the data, but they are subtracted out by first collecting data when bubbles are not being added to the flow, and then collecting data while bubbles are being added. Subtracting the first spectrum from the second yields a spectrum of bubbles only.

BUBBLE GENERATOR

Simply injecting air into a pipeflow typically makes bubbles in the millimeter size range. Instead of using this technique, water is

supersaturated with air in a pressure vessel at 4 atmospheres pressure and the pressurized water is injected through a petcock valve into the incoming flow just upstream of the pump. The high shear stresses in the valve create large concentrations of small bubbles that have peak concentrations in the 20-50μm diameter range. The overall concentration is controlled by adjusting the flowrate of the bubbly water going into the pipe.

During the tests, the flowrate of the bubble water is monitored with a flowmeter to insure that the bubble injection remains constant during the collection of the intake and exit bubble spectra.

AIR CONTENT MEASUREMENT

The total air content of the water is measured with a Van Slyke Blood Gas Apparatus. This device extracts the air dissolved in 10 cm^3 of water by vacuum deaeration and then measures the pressure of the extracted air in a 2 cm^3 volume. The pressure indicates how much air is dissolved in the water, and the results are expressed as percent saturation of the water sample at the sample temperature and one atmosphere pressure. Typically three air content readings were averaged per test.

TEST PROCEDURE

The water in the tunnel is prepared by filtering and adjusting the air content to the appropriate value. The pipe system pump is turned on and the flow is adjusted via the control valves and bypass pipe to the desired flow speed. The pressure is adjusted by either adjusting the control valves or by pressurizing the water tunnel, and the flow through the bubble detector is set to about 10% or 40% of the main pipe flow.

With everything at the proper condition but the bubble generator turned off, a spectrum is recorded in the bubble detector to measure particles or any stray cavitation bubbles that would also show

up in the spectrum with bubble injection. Then the bubble injection is started and the bubble injection rate is adjusted by visually examining the signals on an oscilloscope. A second spectrum is recorded and the first one is subtracted from it in the pulse height analyzer. This creates the intake bubble spectrum.

Immediately after the second spectrum is measured, the valves are switched to bypass about 10% or 40% of the flow leaving the main pipe through the bubble detector. The net flow through the main pipe is kept constant by bypassing some of the upstream flow through the tee just downstream of the pump. This compensates for the increased pipe flow that would otherwise result from only closing the upstream bypass to the detector. The flow through the detector is kept constant by monitoring the detector velocity from the two optical channels and making adjustments as necessary. This maintains a constant flow through the pump to assure constant bubble concentration. When everything is set, the third spectrum is recorded. Afterwards the bubble injection is stopped and a fourth spectrum is recorded and subtracted from the third to insure that the exit spectrum is only bubbles.

The net intake and exit spectra are compared to derive the net mass transfer coefficient.

For the two higher Reynolds number tests, 10% of the main pipe flow was bypassed for bubble counting. This was enough to count large numbers of bubbles in a short time. At the slow speed, however, 40% of the flow was required to obtain sufficient data in a short time.

ASSUMPTIONS AND APPROXIMATIONS

The most significant assumption of this experiment is that the bubbles injected into the entrance of the pipe section do not breakup or coalesce as they pass through the pipe. Consequently the bubble concentrations remain constant and differences between the intake and exit bubble spectra can result only from changes in bubble size. A simple way to examine the assumption of constant bubble concentration with no breakup or coalesence would be to generate an initial bubble distribution that had a peak concentration in the middle

of the size range or some other easily identified spectral characteristic. If the exit spectrum had the same shape as the intake spectrum but was shifted to a smaller size, the constant concentration assumption would be proven. Unfortunately, the spectra generated by the bubble generator, after going through the pump, usually had distributions of decreasing concentration with increasing size, and no distinct spectral features occurred (except for the first test which had a concentration maximum in the middle of the size range). Hence all the assumptions leading to the constant concentration assumption need to be examined in more detail.

BUBBLE BREAKUP

Bubble breakup and deformation are controlled by local shear stresses and surface tension forces which resist deformation. The largest average shear stress τ_w is at the pipe wall. This stress was calculated from the pipe pressure gradient and compared to the surface tension stress τ_σ which resists deformation

$$\tau_\sigma = \frac{\sigma}{2R} \tag{10}$$

for which σ is the surface tension.

For the largest bubbles (170 μm) and greatest value of wall shear stress tested, the ratio τ_σ / τ_w was a minimum of 20. Hence the bubbles should neither breakup nor deform appreciably.

Another way to address bubble breakup or deformation is through the Weber number, in this case the ratio of the dynamic head of the microscale eddies multiplied by the bubble diameter divided by the surface tension. This number ranged from order 10^{-1} for the largest bubbles at the highest Reynolds number test to 10^{-4} for the smallest bubbles at the lowest Reynolds number. In this range bubble splitting and deformation should not occur.

BUBBLE COALESENCE

The assumption that the bubbles do not coalesce was tested by running a high concentration bubble spectrum through the pipe at essentially saturated conditions. If coalesence were to occur, the overall concentration at the pipe exit would be less than that at the pipe entrance. If the concentrations of small bubbles in the intake spectrum were not significantly larger than those of the large bubbles, bubble breakup would result in a shift in the exit spectrum of large size bubbles to many smaller ones. This test (Test 1), with an initial concentration of 35 bubbles/cm^3, shows no coalesence or breakup. See Figure 4. The intake and exit spectra are similarily shaped. The exit spectrum is shifted along the size axis to a slightly larger size as expected from the slight level of oversaturation. All other tests in this investigation used much lower bubble concentrations. Hence they would also not suffer from coalesence effects. See Table 1.

APPROXIMATIONS

The parameters that define the mass transfer coefficient in Equation 4 are approximated in this experiment as being constant, but they do vary somewhat. The actual air saturation level in the pipe is dependent on the local pipe pressure which varies along the pipe because of the pressure gradient. Because the net change in bubble size is all that can be measured, the average saturation value is used in defining the transfer coefficient. This approximation is the main compromise of using an out-and-back pipe flow design but it produces a tolerable error. The worst cases occured in the high Reynolds number tests which had the greatest pressure gradient. In those tests the saturation levels changed 30% of the mean value from one end of the pipe to the other. The lower Reynolds number tests had changes of saturation level that were 10% or less of the mean value.

The air density ρ_g also changes because of pressure loss along the pipe and surface tension pressure changes in the shrinking bubble, but these changes are small throughout the bubble dissolving history. The

magnitude of the second term in Equation 3 ($\frac{4}{3}pR^3\frac{dr_s}{dt}$) that contains the time derivative of density was estimated and it is at most 8% of the magnitude of the first term for one third of the tests and 3% or less for the other tests. This term was therefore ignored and the air density is approximated as being constant.

The surface tension pressure was about 10% of the total bubble pressure for the smallest bubble sizes during most of the tests in the experiment, and this contribution decreased quickly with larger bubbles. For simplicity the surface tension pressure was therefore ignored in the calculations of air saturation levels.

Air is used as the dissolved gas in this experiment for simplicity and is approximated as a pure substance. Because turbulent transport processes should control the dissolving, the differences in the molecular diffusivities and solubilities of oxygen and nitrogen should cause negligible effects. This allows the air mixture to be reasonably approximated as a pure substance whose properties are calculated based on oxygen and nitrogen values weighted according to their molar fractions.

UNCERTAINTY ESTIMATES

The uncertainty interval for the mass transfer coefficient can be estimated by looking at the uncertainties of the parameters used to define it. These uncertainties are those of the actual measurements themselves, not the uncertainties made by assumptions or approximations.

Referring to Equation 4, the mass transfer coefficient depends on the non-dimensional air saturation level, $\rho_s/(c_s - c_\infty)$, the elapsed bubble dissolving time, Δt, and the change in bubble size, ΔR. The first term depends on tabulated solubility values, the perfect gas law, Henry's Law, and the accuracies of the Van Slyke apparatus and the differential pressure gage. These latter two instruments were calibrated or checked and were within 2% of their calibration values. The solubilities and

physical laws are also of similar accuracy. The elapsed time, Δt, depends on the length of PVC tube, the differential pressure reading and the relation of pressure drop to velocity as shown in Equation 5. The tube length was measured and Equation 5 was derived from experimental measurements that match to within about 2% for the Reynolds numbers of the flows. The elapsed flow time was also cursorily checked by injecting dye and clocking the time for the dye to transit the tube. The elapsed time should be correct within 2% of its value.

These errors are less significant than uncertainties from the bubble measuring process. The detector accuracy is roughly 4μm over the range of bubble diameters measured (see Figure 3), and this is somewhat significant compared to some of the measured radii changes, ΔR. See Table 1. The most significant uncertainty, however, is the statistical variation in bubble concentration when the actual number of bubbles counted in a particular size band is low. With low count values, the interval of concentration for a given confidence level that contains the true average concentration becomes significant when compared to the concentration itself. To illustrate this, Test 6 was replotted with 80% confidence intervals on concentration for the two spectra. The spectra were also smoothed. See Figure 5. The confidence interval was calculated by assuming the bubbles to be Poisson distributed in space and using the statistical technique outlined in Reference 9. The uncertainties of the bubble concentrations become uncertainties of bubble size changes when graphically measuring the shift of the spectrum along the size axis, ΔR. For this typical test, the size change varied ±10% to ±15% of its mean value. This variation is always a minimum at the smaller sizes because the numbers counted at those sizes are the greatest and yield the least variation of concentration. When the data are reduced, the measured size changes are weighted by the concentration of bubbles in the analyzed concentration band. Hence, the larger variations in size change that occur for the larger bubbles do not affect the data very much. The exact form of the data reduction is listed in the Data Reduction Section. The net effect of this uncertainty phenomenon is to make the mass transfer coefficients accurate to nominally ±10% to ±15%, and this uncertainty

is larger than the others.

DATA REDUCTION

The bubble data are counted in discrete voltage (size) bins in the pulse height analyzer. The counts in each bin are then divided by the size bandwidth of the bin and the total volume of water illuminated by the bubble detector. This volume is simply the detector sampling area multiplied by the average bubble velocity in the detector and the elapsed data collection time. The results from each bin are plotted at the bin's center diameter to create a bubble concentration versus size distribution or spectrum. The narrowest bins are 5 μm wide at the highly concentrated smaller sizes and 20 μm wide at the less concentrated larger sizes.

The size shift of the spectra is measured by weighting the size shift in small increments of concentration by the total concentration of bubbles at that concentration band. That is,

$$\Delta R = \frac{\sum^{i} (n_{i+1} - n_i)(d_{i+1} - d_i)\Delta R_i}{\sum^{i} (n_{i+1} - n_i)(d_{i+1} - d_i)} \tag{11}$$

Because no consistent variation of bubble size change as a function of bubble size was observed, the above reduction technique was applied to the entire exit bubble spectra. Because the smaller bubbles of the intake spectra usually dissolved to a size below the detection threshold of the detector, they are not included in the data reduction.

Diameter variations of the flexible PVC tube caused by varying test pressure changes are accounted for when calculating pipe velocities or Reynolds numbers.

RESULTS

The nine pairs of test spectra are shown in Figure 6 The exit spectra are typically shifted from the intake spectra parallel to the size axis except for Tests 4 and 8, and these tests show opposite trends of a dependency of bubble dissolving, as evidenced by bubble diameter reduction, on bubble size. Hence the spectra indicate that the bubble dissolving rates or mass transfer coefficients are essentially independent of bubble size, over the range measured, for a given set of flow conditions. This result allows each test's data to be reduced to an average bubble radius reduction via Equation 11, and the mass transfer coefficients are calculated according to Equation 4.

These coefficients are shown in Figure 7 as a function of Reynolds number. The coefficients repeat reasonably well and show no variation with gas saturation level. The coefficients' variance with respect to their mean at each Reynolds number is 9% to 18% of mean value. The coefficients increase with pipe Reynolds number and this increase is approximately linear. Mass transfer would be expected to increase with turbulence level.

COMPARISON OF RESULTS TO THEORETICAL PREDICTIONS

The diffusion equation (Fick's Law) has been solved to predict the gas diffusion out of stationary bubbles, bubbles with fluid or rigid (surfactant coated) surfaces rising irrotationally under their own buoyancy, and bubbles in isotropic, turbulent flow. The solutions for irrotationally rising bubbles are limited to small bubbles whose terminal velocities are well-predicted by Stokes' Law, typically 160 μm in diameter or less for air bubbles in water. For bubbles suspended in turbulent flow, the local flow around the bubble is usually assumed to be Stokes-like. The diffusion rates may be non-dimensionalized in the form of a Nusselt number which compares the mass flow rate out of the bubble to the flow rate caused by molecular diffusion alone.

$$Nu = \frac{-dm/dt}{4\pi RD(c_s - c_\infty)} \tag{12}$$

in which $-dm/dt$ is the mass transfer rate out of the bubble, R is the radius, D is molecular diffusivity and $(c_s - c_\infty)$ is the difference in concentration potential.

The Nusselt number (Nu) for rising bubbles is typically dependent on the Peclet number (Pe) which compares the bubbles' convective diffusivity (UR) to its molecular diffusivity (D).

$$Pe = \frac{UR}{D} \tag{13}$$

The velocity used to define the Peclet number depends on the flow regime of interest. For bubbles rising at terminal velocity,

$$Pe_R = \frac{U_T R}{D}, \qquad U_T = \frac{gR^2}{3\upsilon} \quad \text{(fluid surface bubbles)} \tag{14a1}$$

$$U_T = \frac{2gR^2}{9\upsilon} \quad \text{(rigid surface bubbles)} \tag{14a2}$$

in which U_T is the terminal velocity.

For bubbles suspended in turbulence,

$$Pe_T = \frac{U_e R}{D}, \qquad U_e = \frac{R\varepsilon^{1/2}}{\upsilon^{1/2}} \tag{14b}$$

in which U_e is a turbulence velocity scale and ε is the local energy dissipation rate.

Various relationships between the Nusselt and Peclet numbers have been derived or measured. For stationary bubbles which dissolve purely by molecular diffusion, Epstein and Plesset (1950) derived the result

$$Nu = 1.0 \qquad (Pe = 0) \tag{15}$$

For small, fluid surface bubbles rising at terminal velocity, the relation derived by Levich (1962) is

$$Nu = \left(\frac{2}{3\pi}\right)^{1/2} Pe_R^{1/2} \tag{16}$$

For similar bubbles with rigid surfaces, such as surfactant coated bubbles,

$$Nu = \left(\frac{2}{\pi}\right) Pe_R^{1/3} \tag{17}$$

Batchelor (1980) derived a theoretical prediction for mass transfer from a rigid surface bubble or particle suspended in locally isotropic turbulence,

$$Nu = 0.55 Pe_T^{1/3} \tag{18}$$

He shows that if the bubbles or particles are about the same size or smaller than the smallest turbulent eddy scales, the only fluid motion that contributes to the mass transfer is the relative motion of the fluid near the bubble or particle surface during eddy straining from vorticity. Induced velocities from density differences or accelerations contribute to dissolving only if there is a net component of these velocities parallel to the average vorticity direction. Because small eddies are often statistically isotropic even in globally non-isotropic flows, the bubble- or particle-induced velocities do not affect the dissolving rates averaged over time. Consequently, the mass diffusion depends only on the straining rates of the small eddies. For rigid surface bubbles or particles, Batchelor shows that the resulting Nusselt number from eddy straining depends on the cube root of the Peclet number. For fluid surface bubbles or droplets, Gupalo and Ryazantsev (1972) show that eddy straining diffusion results in a Nusselt number that is proportional to the square root of the Peclet number,

$$Nu \alpha Pe_T^{1/2} \tag{19}$$

If the bubbles in this experiment are similar in size to the small scale eddies in the pipe flow, and these eddies are roughly isotropic, then Equation 19 will best approximate the Nusselt number result for pipe flow dissolving.

The measured spectra of Figure 6 show no clear dependency of dissolving rate on bubble size as evidenced by the parallel shift of the intake and exhaust spectra. From the definitions of the mass transfer coefficient, Nusselt number and Peclet number in Equations 4, 12 and 14b, it can be shown that the Nusselt number must vary with the Peclet number to the one-half power for the observed bubble dissolving rate to be independent of size as observed in the present experiment. Hence the results support the theoretical relation of Equation 19 for mass transfer from fluid surface bubbles.

The data can be reduced into a non-dimensional Nusselt number using the Peclet definition given in Equation 14b and using the previously discussed square root relationship. The empirical result is

$$Nu = 0.12 Pe_T^{1/2} \tag{20}$$

This equation is listed in Table 2 for comparison to the Nusselt numbers of stationary and rising dissolving bubbles. The results are also plotted in non-dimensional form in Figure 8 over the range of bubble radii actually measured.

Although the results show the mass transfer coefficient to be roughly independent of size as predicted by Equation 19, the magnitudes of the coefficents are not much greater than those of the other dissolving regimes listed previously. They are in the same range as the coefficients for bubbles buoyantly rising at terminal velocity. See Table 2. This is unexpected because one would assume the turbulence in the pipe would significantly increase the mass transfer rate over that of a rising bubble. An explanation for the lower diffusion rates in the pipe flow is bubble rotation. The rising bubble prediction assumes no

bubble rotation. Any rotation will "wrap" the diffusion boundary layer flow around the bubble and reduce the flushing action of the local external flow. This suppression of diffusion by rotation was mentioned in Reference 4 regarding particle diffusion in a turbulent stream. If a particle were settling in a still tank, the diffusion from the particle would decrease with the addition of gentle mixing and subsequent particle rotation. The diffusion would go through a minimum as the mixing began and the flux would change from that predicted by Equation 17 to that predicted by Equation 18 This is difficult to prove without more experimentation but qualitatively the present results would support that idea.

Another interesting result from the Nusselt number formulation is that the measured numbers are less than unity at the lowest Reynolds number tested, yet the Nusselt number for the slowest dissolving regime, molecular diffusion, is unity. The reason for the discrepancy is believed to be surfactant contamination. Trace surfactants will adsorb onto a bubble's air interface and occupy sites on the bubble that would otherwise be occupied by water molecules. As the surfactant molecules pack more tightly at higher concentrations, they form patches or micelles that reduce the area through which dissolving can occur. Over a wide range of surface densities of surfactant molecules, the bubble surface area available for diffusion can be significantly reduced yet still remain mobile. The point at which the bubble surface becomes a rigid skin represents a very high surfactant density on the surface. Any surfactant contamination in the water could reduce the dissolving rate proportional to the reduced surface area available for mass transfer.

A cursory check of the surfactants in the water was made by blowing bubbles into a sample of the tunnel water and seeing how long a bubble would last on the surface. In clean water, a bubble will burst almost immediately, whereas in contaminated water a bubble may last for several seconds. The bubbles in this case lasted between 1 to 7 seconds which indicates that the water was not surfactant-free. Also, previous measurements of bubbles dissolving via molecular diffusion in similar water resulted in Nusselt numbers around 0.5 to 0.7, not 1.0 (Reference 10). The minimum Nusselt numbers in Figure 7 in the

present case are about in this range, hence surfactants are believed to cause these latter numbers to be lower than expected.

CONCLUSIONS

Bubble dissolving in a turbulent flow can be adequately measured with an out-and- back type pipe arrangement using a single bubble detector. The mass transfer coefficient for the bubbles can be determined and the variation of this coefficient with bubble size can be resolved.

The mass transfer coefficient is independent of bubble size in the 20μm to 170μm diameter range. Consequently the mass transfer Nusselt number varies with the square root of the turbulent Peclet number.

The mass transfer coefficient increases with the flow Reynolds number and the values are similar, at Reynolds numbers of 10^4 to 10^5, to theoretical mass transfer coefficients for buoyantly rising bubbles that are the same size. However the measured values may be low because of surfactant contamination.

THIS PAGE

INTENTIONALLY

LEFT BLANK

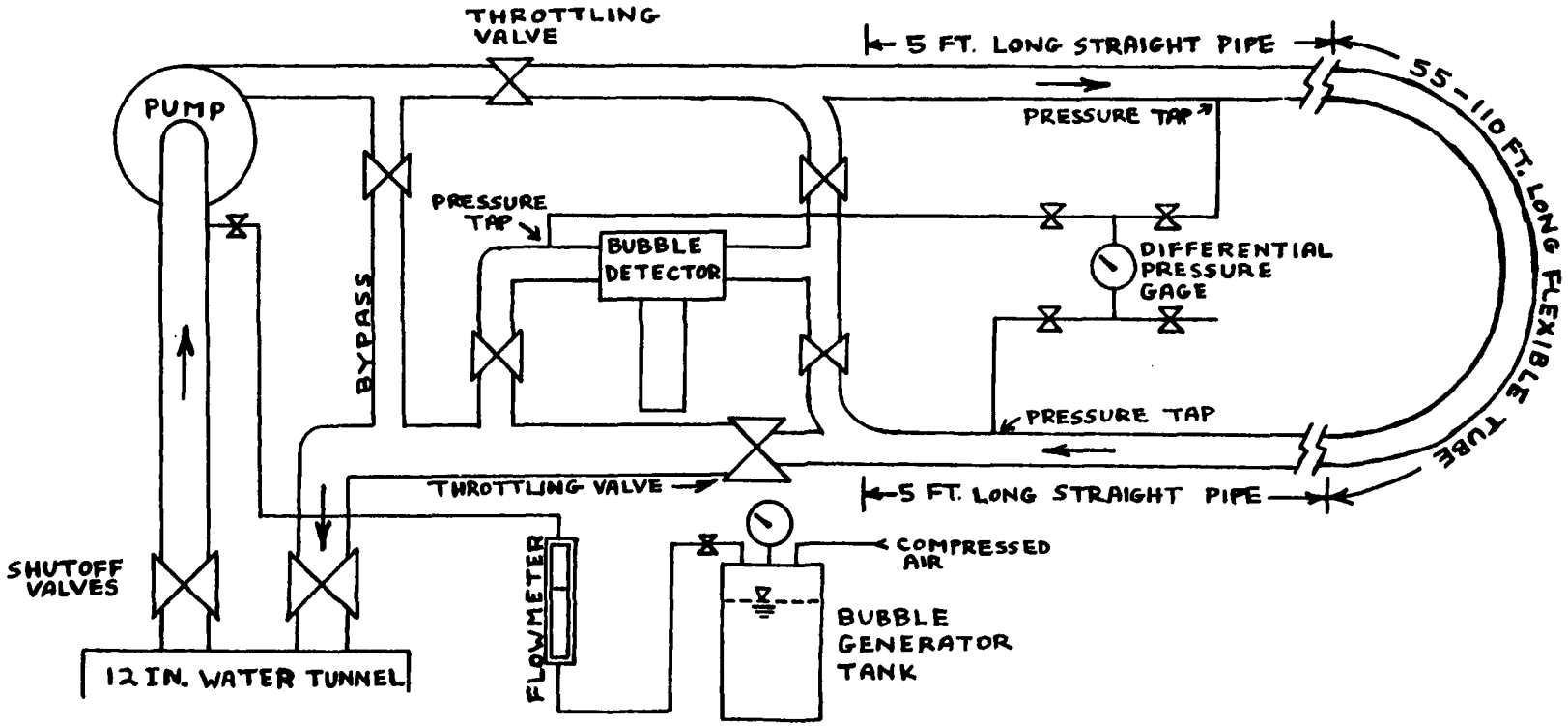

Pipe Flow Facility
Figure 1

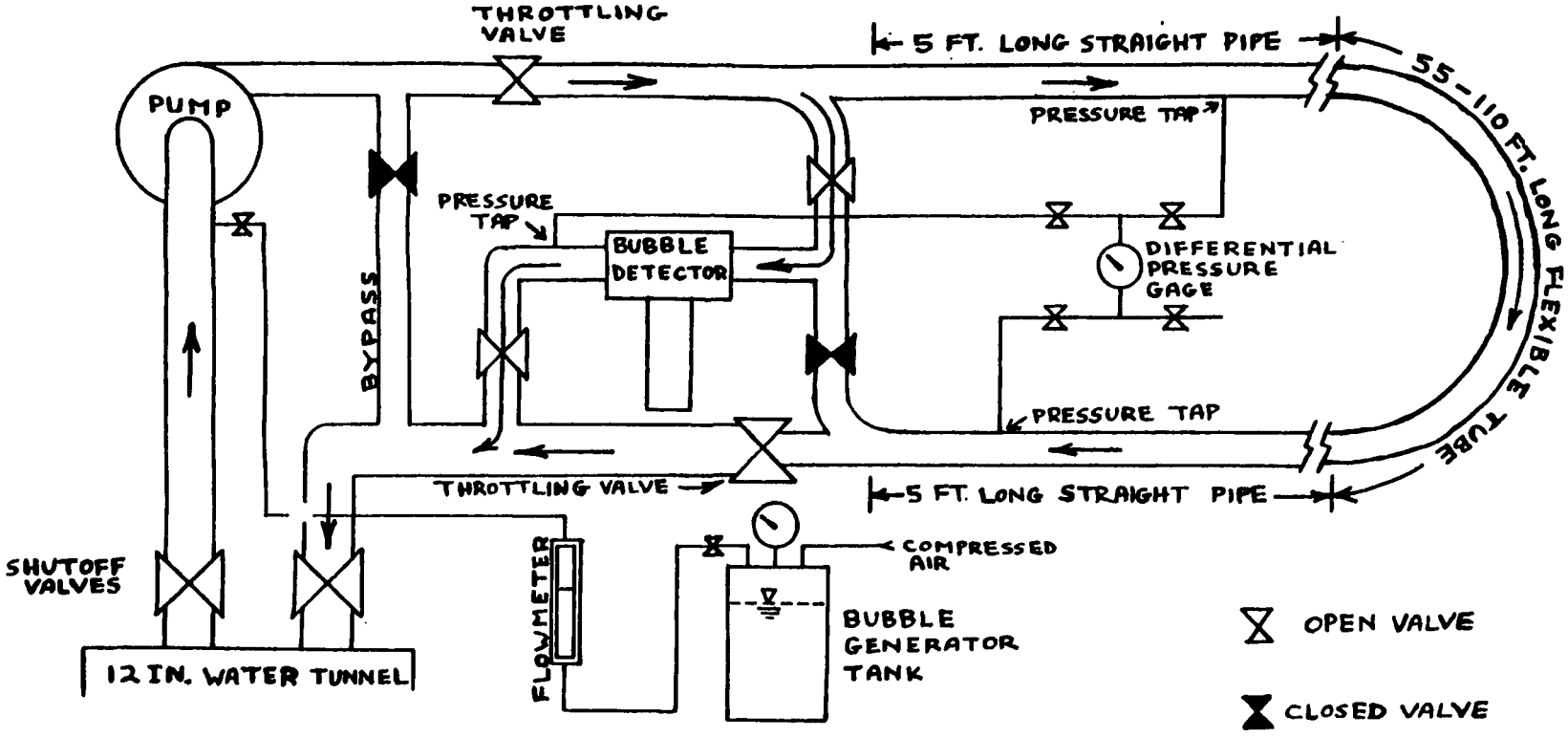

Pipe Flow Facility--Bubble Intake Spectrum
Figure 1a

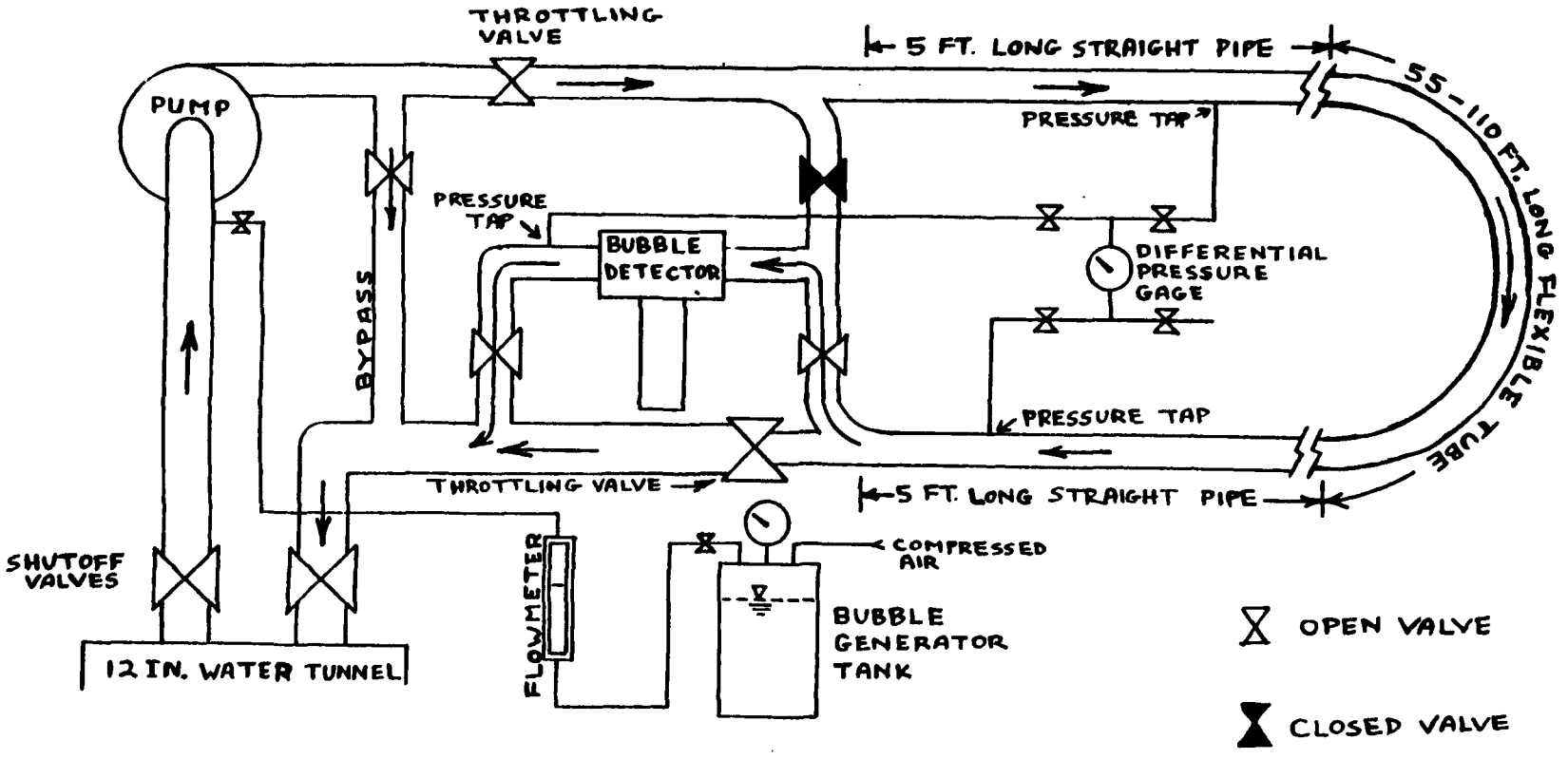

Pipe Flow Facility—Bubble Exit Spectrum
Figure 1b

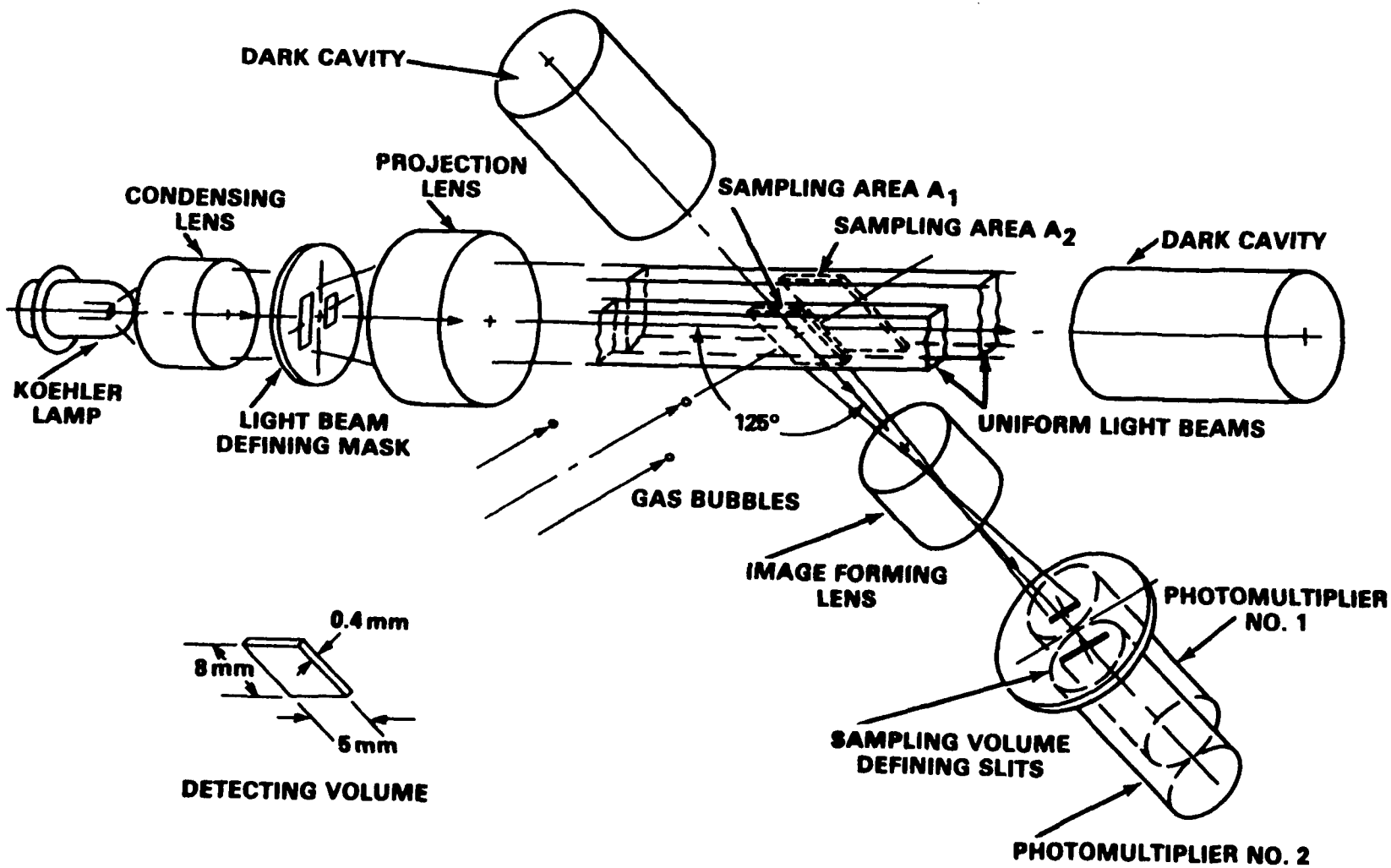

Bubble Detector Schematic

Figure 2

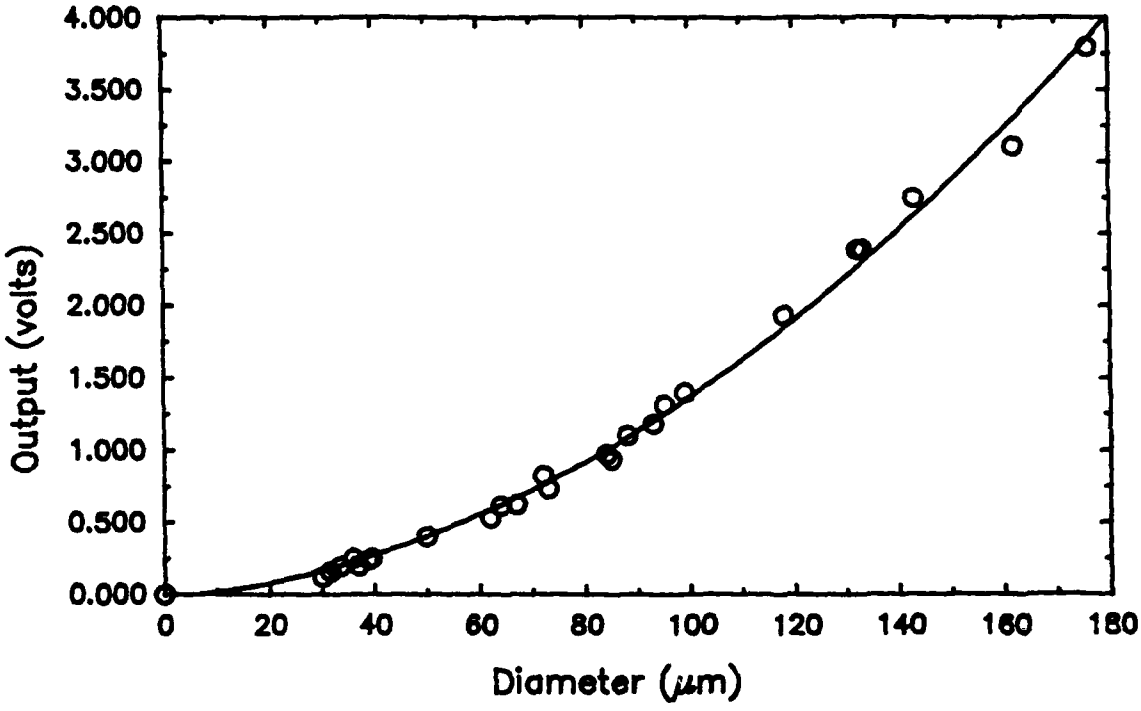

Bubble Detector Calibration

Figure 3

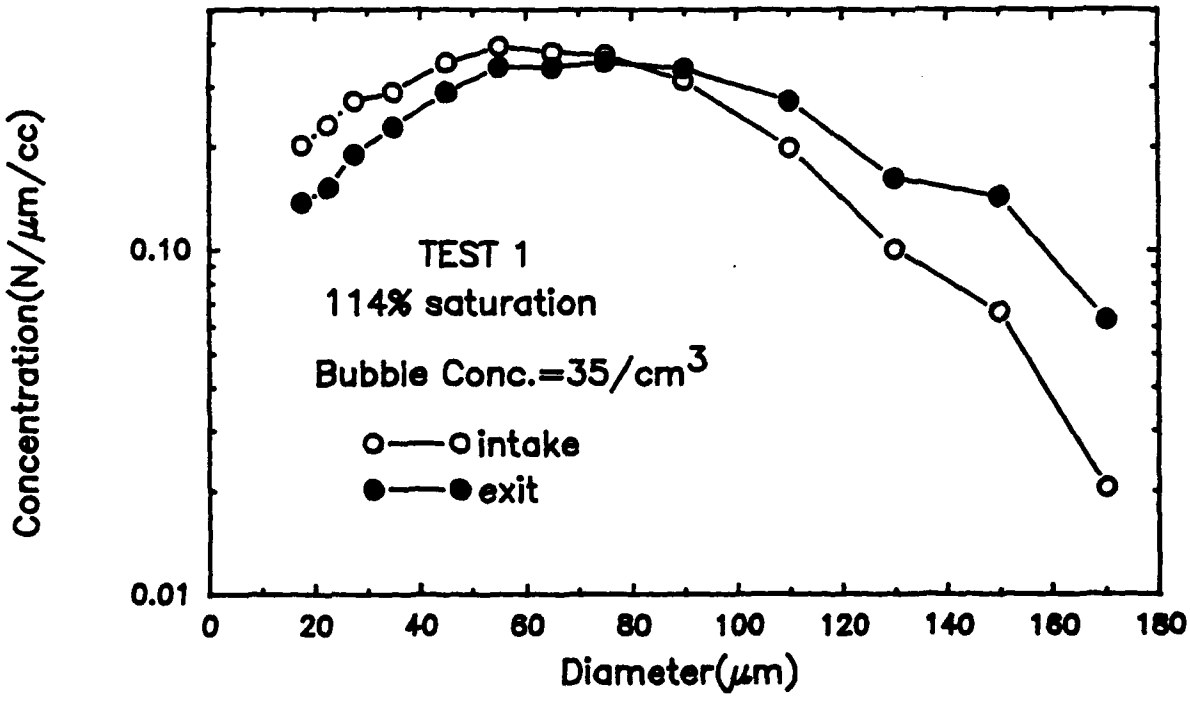

TEST 1

Figure 4

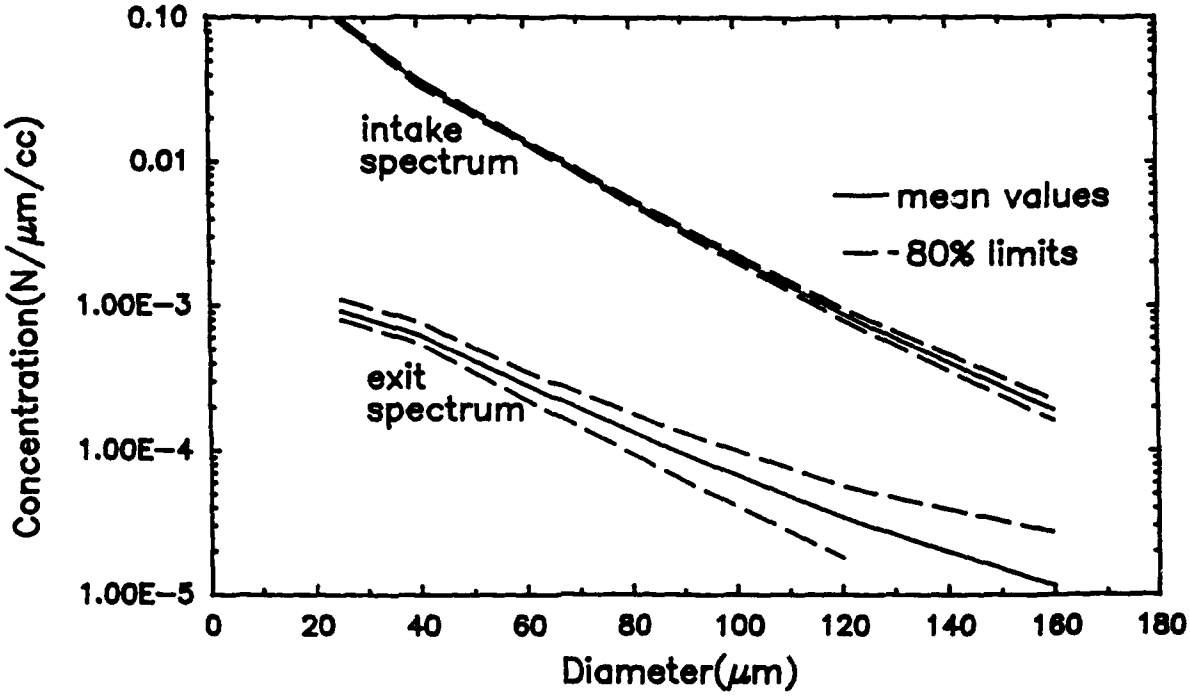

Typical 80% Confidence Intervals of Concentration

Figure 5

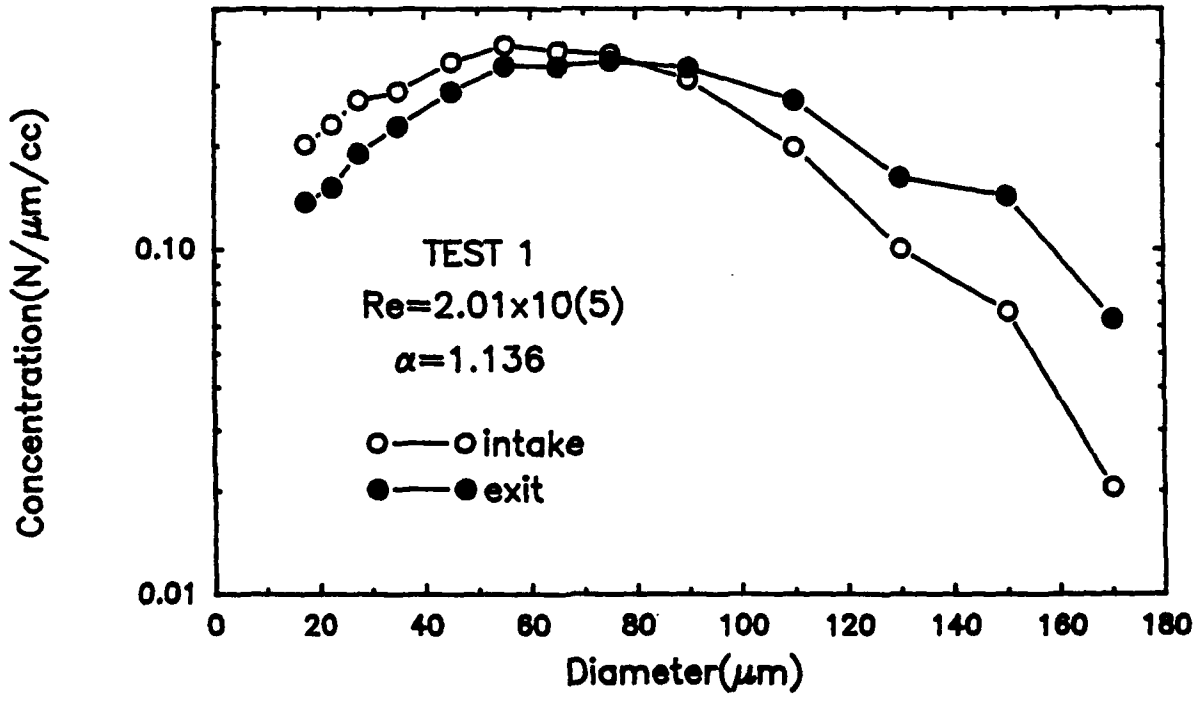

TEST 1

Figure 6a

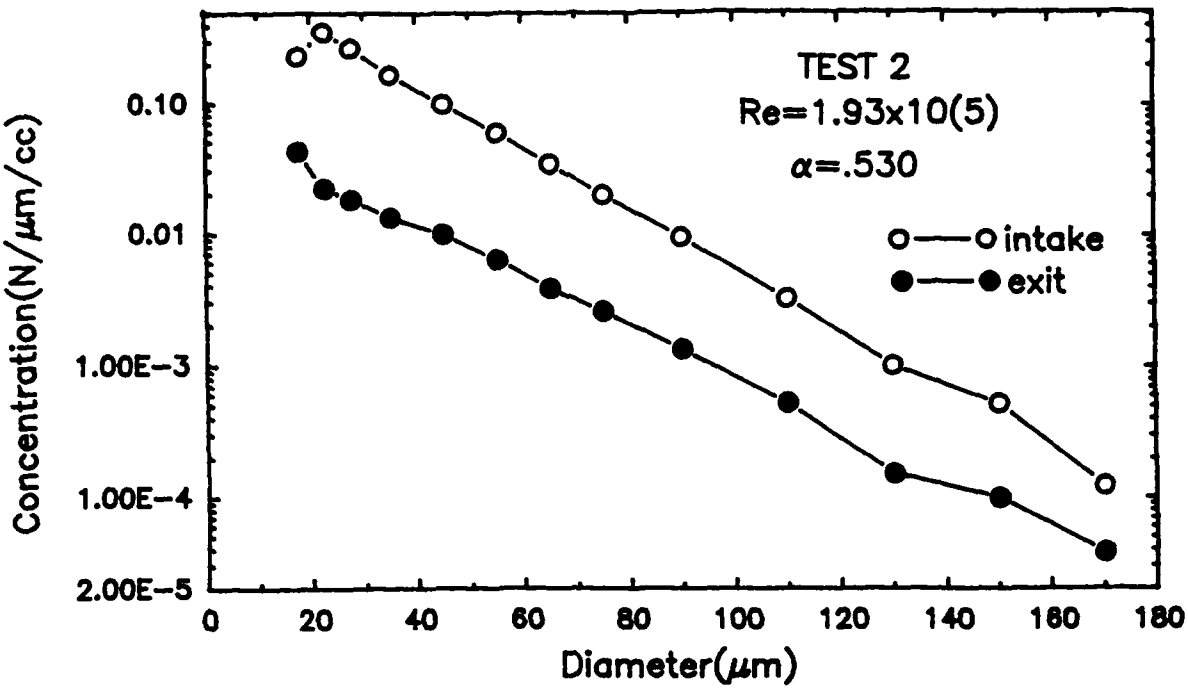

TEST 2
Figure 6b

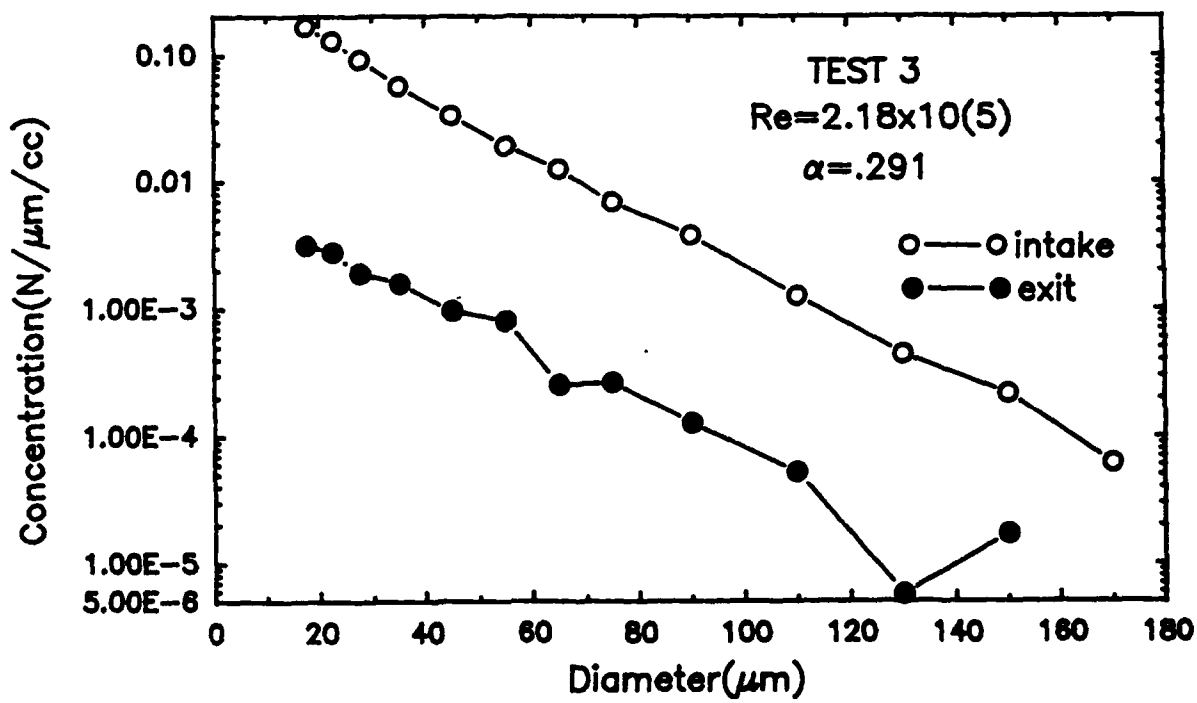

TEST 3
Figure 6c

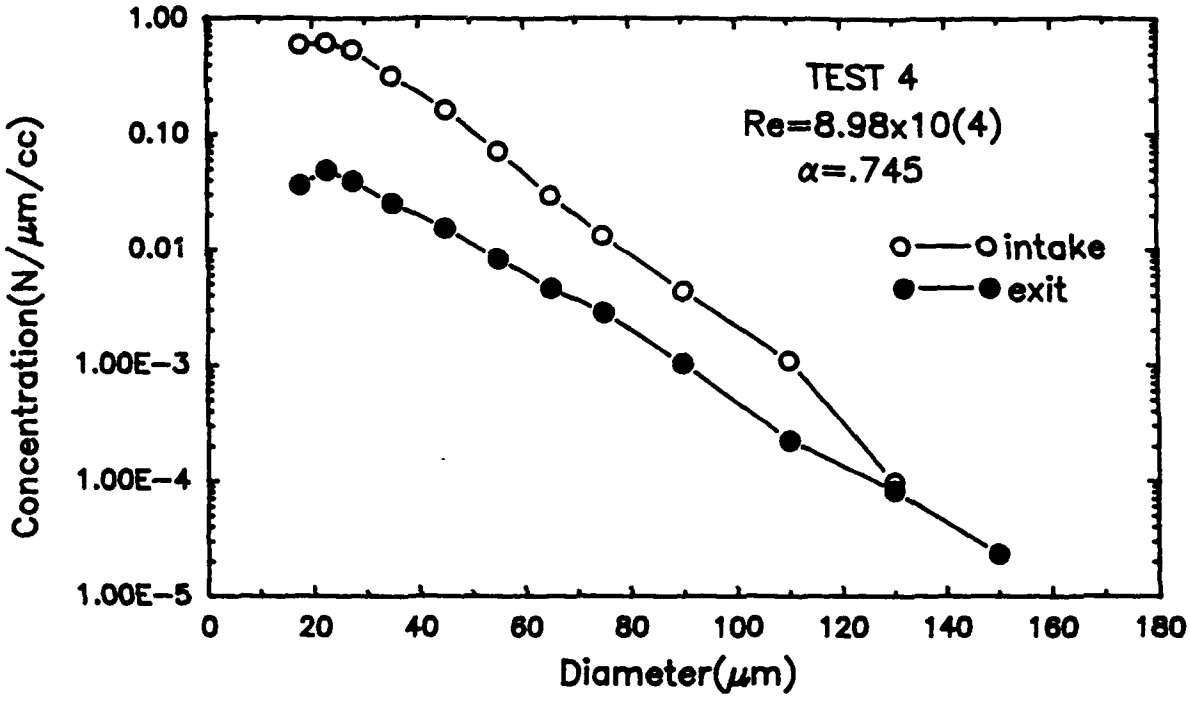

TEST 4

Figure 6d

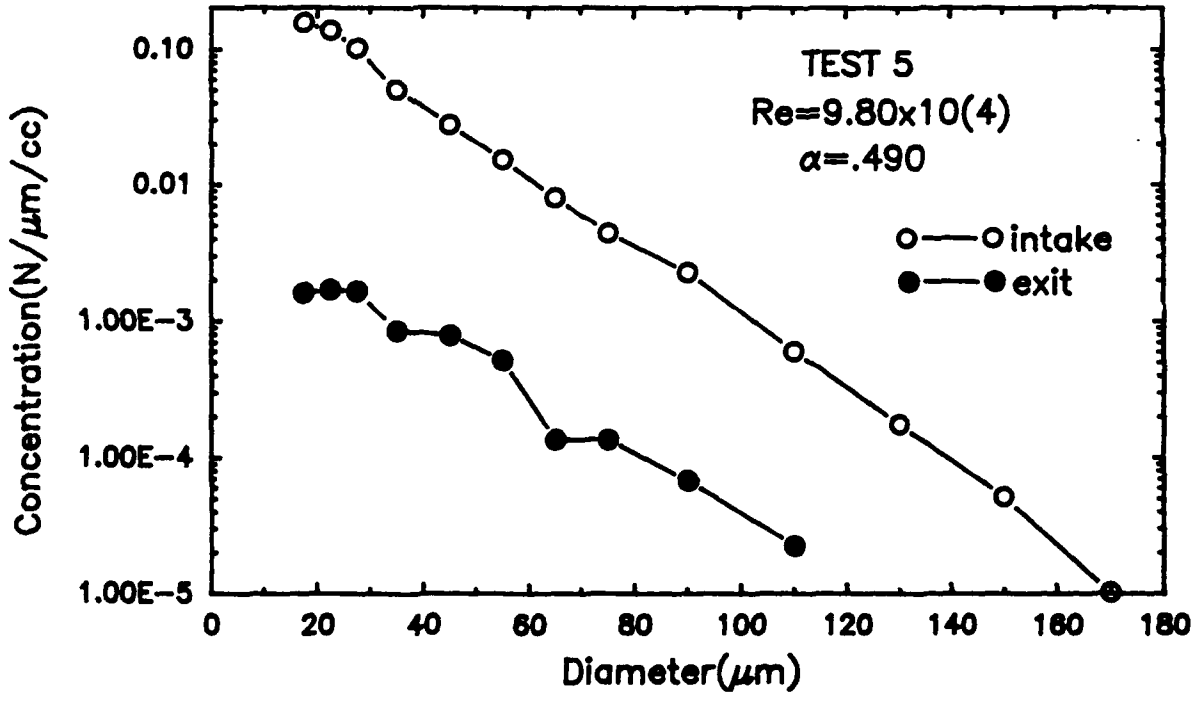

TEST 5

Figure 6e

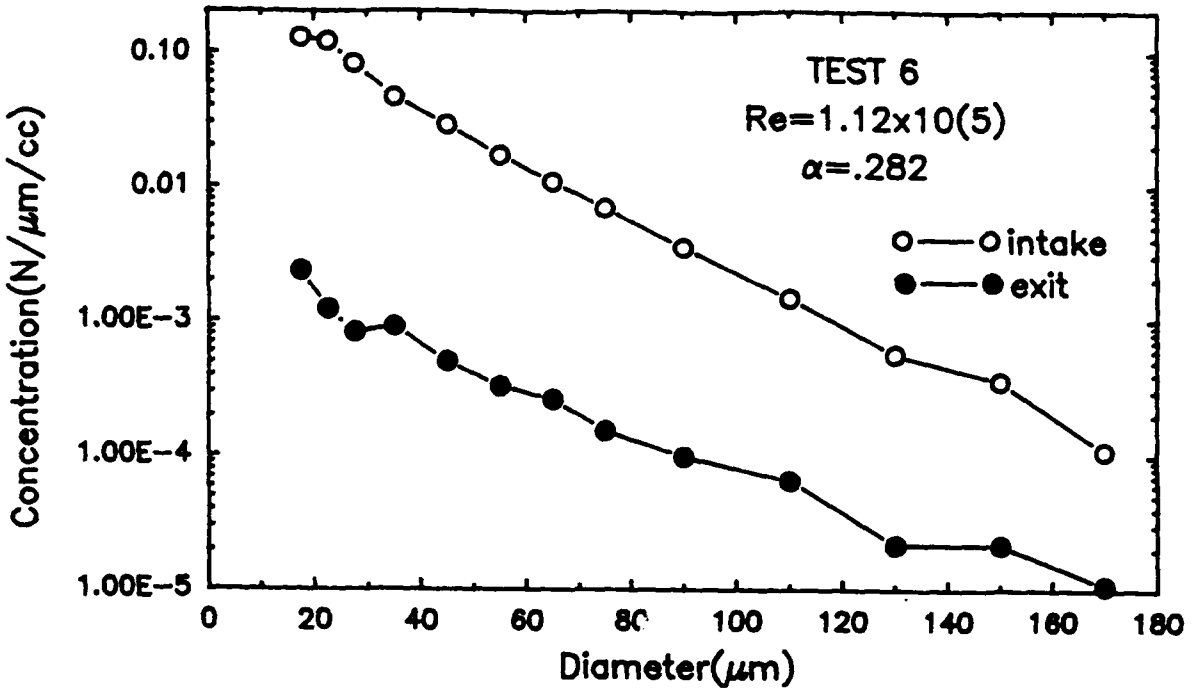

TEST 6
Figure 6f

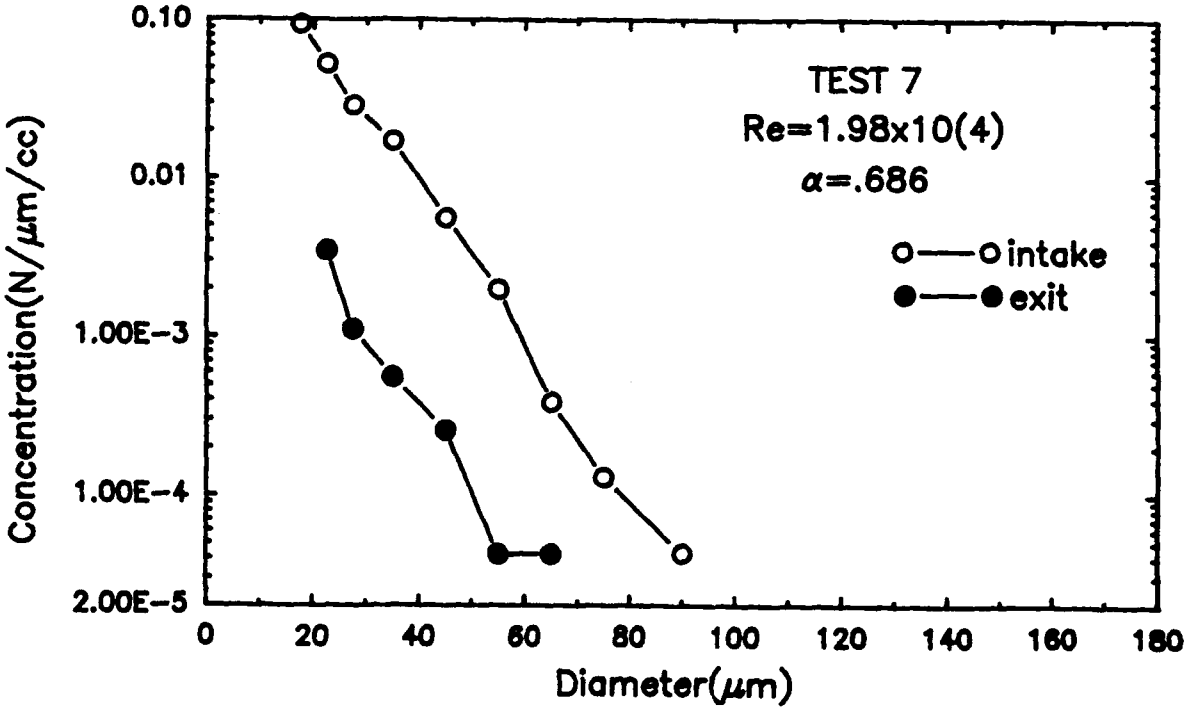

TEST 7
Figure 6g

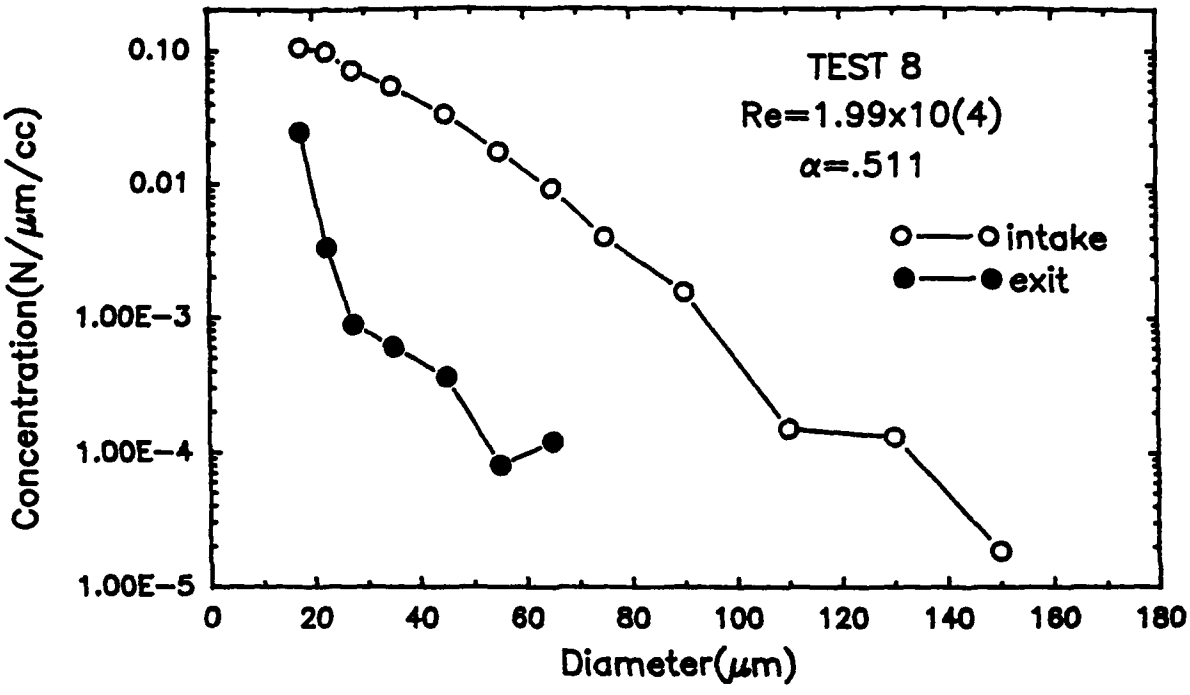

TEST 8

Figure 6h

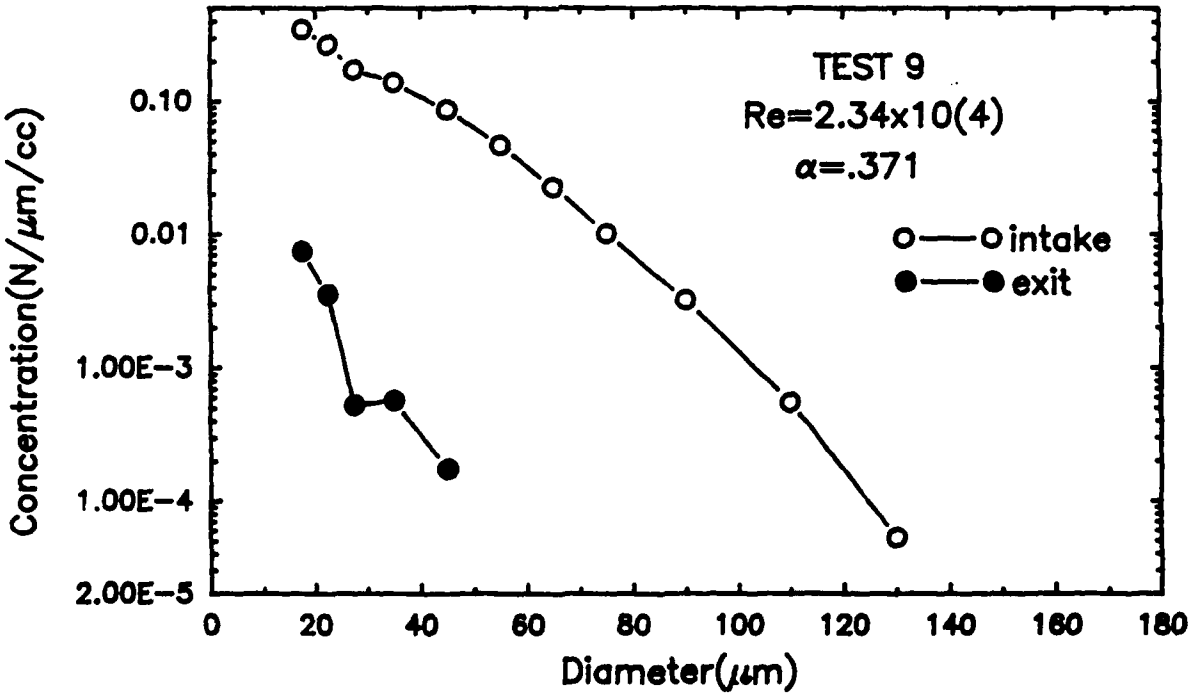

TEST 9

Figure 6i

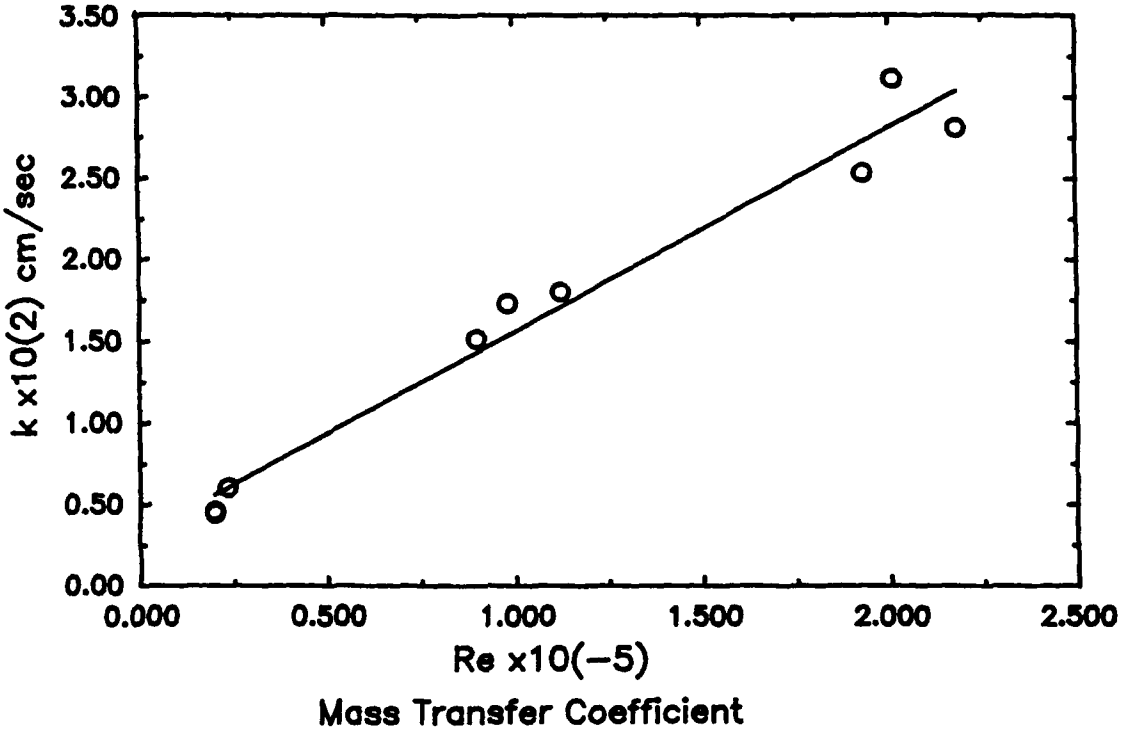

Mass Transfer Coefficient

Figure 7

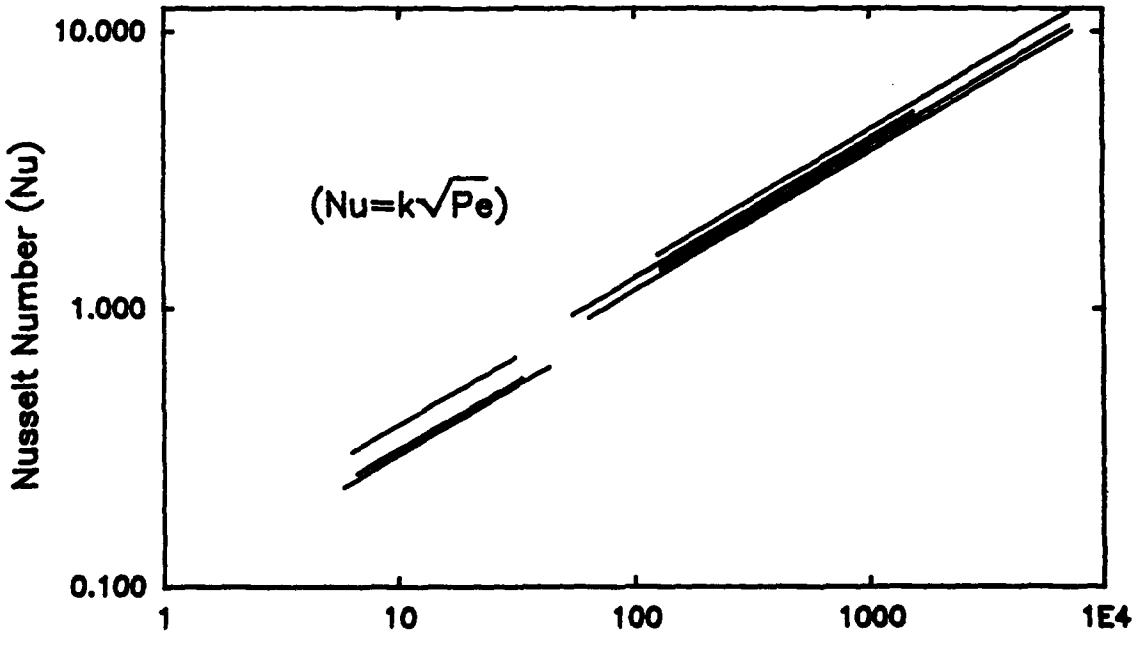

Range of Measured Nusselt and Peclet Numbers

Figure 8

TEST NUMBER	1	2	3	4	5	6	7	8	9
dP/dx (dynes/cm^3)	166	162	166	56.0	53.8	51.7	3.21	3.33	3.17
α_{attn}	1.780	0.865	0.578	1.045	0.735	0.722	0.898	0.664	0.687
$\overline{\alpha}$	1.136	0.530	0.291	0.745	0.490	0.282	0.686	0.511	0.371
ΔR (μm)	7.85	22.5	35.6	15.1	32.2	44.8	14.2	21.1	33.2
n_o (cm^{-3})	35.2	8.38	3.35	14.9	3.10	2.88	1.13	2.59	7.04
Re_p	2.01×10^{5}	1.93×10^{5}	2.18×10^{5}	8.98×10^{4}	9.80×10^{4}	1.12×10^{5}	1.98×10^{4}	1.99×10^{4}	2.34×10^{4}
k (cm/s)	3.11×10^{-2}	2.53×10^{-2}	2.81×10^{-2}	1.51×10^{-2}	1.73×10^{-2}	1.80×10^{-2}	4.55×10^{-3}	4.41×10^{-3}	6.00×10^{-3}
$Nu/Pe^{1/2}$	0.139	0.117	0.121	0.116	0.125	0.129	0.0985	0.0943	0.120

Table 1.

TEST PARAMETERS

STATIONARY BUBBLES	BUBBLES RISING AT TERMINAL VELOCITY		TURBULENT FLOW
	MOBILE SURFACE (CLEAN)	RIGID SURFACE (DIRTY)	CONCECTING BUBBLES (PRESENT RESULTS)
$Nu = 1.0$ $(Pe = 0)$	$Nu = \left(\frac{2}{3\pi}\right)^{1/2} (Pe)^{1/2}$ $Pe = \frac{9R^3}{3\nu D}$	$Nu = \left(\frac{2}{\pi}\right)(Pe)^{1/3}$ $Pe = \frac{2gR^3}{9\nu D}$	$Nu = 0.12(Pe)^{1/2}$ $Pe = \frac{\varepsilon^{1/2} R^2}{\nu^{1/2} D}$
$k = D/R$	$k = \frac{1}{3}\left(\frac{2gD}{\pi\nu}\right)^{1/2} R^{1/2}$	$k = \left(\frac{2}{\pi}\right)\left(\frac{2gD^2}{9\nu}\right)^{1/3}$	$k = 0.12\left(\frac{\varepsilon}{\nu}\right)^{1/4} D^{1/2}$
$10\mu m < R < 80\mu m$ $0.002 < k < 0.018$	$10\mu m < R < 80\mu m$ $0.011 < k < 0.031$	$10\mu m < R < 80\mu m$ $k = 0.012$	$10\mu m < R < 80\mu m$ $0.004 < k < 0.031$

Table 2.

BUBBLE DISSOLVING RELATIONS

REFERENCES

1. Epstein, P.S., and Plesset, M.S. "On the stability of gas bubbles in liquid solutions," Journal of Chemical Physics, Vol.18, No.11, 1950.

2. Levich, V.G. Physicochemical Hydrodynamics, Prentice-Hall, Inc., Englewood Cliffs, N.J., 1962.

3. Levins, D.M., and Glastonbury, J.R. "Particle-liquid hydrodynamics and mass transfer in a stirred vessel. Part II Mass Transfer," Trans. of the Inst. of Chem. Eng., Vol.50, 1972.

4. Batchelor, G.K., "Mass transfer from small particles suspended in turbulent fluid," Journal of Fluid Mechanics, Vol.98, Part 3, 1980.

5. Gupalo, Y.P., and Ryazantsev, Y.S. "Diffusion on a particle in the shear flow of a viscous fluid. Approximation of the diffusion boundary layer," Appl. Math. and Mech. (P.M.M.), Vol.40, 1976.

6. Froessling, N., Gerlands Beitr. Geophys., Vol.32, No.170, 1938.

7. Schlichting, H., Boundary Layer Theory, 7th. ed., McGraw-Hill Book Co., N.Y., 1979.

8. Hiemenz, P.C. Principles of Colloid and Surface Chemistry, 2nd. ed., Marcel-Dekker, Inc., New York, 1986.

9. Gowing, S. "Comparison of Light Scattering and Holographic Techniques for Bubble and Seston Measurements in a Lake," DTNSRDC/SPD-1236-01, April 1987.

10. Gowing, S. "Dissolving of Bubbles in a Liquid," DTNSRDC-87/006, August 1987.